Nano Energy (2015) 16, 301–309

Available online at www.sciencedirect.com

ScienceDirect

journal homepage: www.elsevier.com/locate/nanoenergy

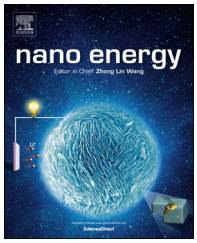

COMMUNICATION

Solution processed flexible hybrid cell for concurrently scavenging solar and mechanical energies

Yuanxing Fang[a,b], Jinhui Tong[a], Qize Zhong[a], Qiao Chen[b], Jun Zhou[a], Qiuping Luo[a,*], Yinhua Zhou[a,*], Zhonglin Wang[c,d], Bin Hu[a,*]

[a]*Wuhan National Laboratory for Optoelectronics, and school of Optical and Electronic Information, Huazhong University of Science and Technology, Wuhan 430074, P.R. China*
[b]*Chemistry Department, School of Life Science, University of Sussex, Brighton BN1 9QJ, UK*
[c]*School of Materials Science and Engineering, Georgia Institute of Technology, Atlanta, GA 30332-0245, USA*
[d]*Beijing Institute of Nanoenergy and Nanosystems, Chinese Academy of Science, Beijing 100083, P.R. China*

Received 8 May 2015; received in revised form 11 June 2015; accepted 18 June 2015
Available online 4 July 2015

KEYWORDS
Hybrid cell;
Solution process;
Silver nanowire;
Triboelectric nanogenerator;
Solar cell

Abstract
Flexible device that can harvest renewable energy from environment is urgently needed nowadays. A satisfactory device should be able to harvest multi-type energies around the clock without any economic difficulties for mass production. Here we report an all solution processed flexible hybrid cell by integrating an organic solar cell and triboelectric nanogenerator into a thin film, which is capable to convert both of the solar and mechanical energies into electric power independently or simultaneously, the generated energy can be used either to charge an energy storage unit or as a primary energy source for wearable self-powered devices even in the weak light conditions. This work provides a feasible and scalable method to fabricate the hybrid energy devices within reasonable cost to overcome the environmental restrictions of the devices that the mode of harvest single energy form.

*Corresponding authors.
E-mail addresses: luoqp@hust.edu.cn (Q. Luo), yh_zhou@hust.edu.cn (Y. Zhou), bin.hu@hust.edu.cn (B. Hu).

http://dx.doi.org/10.1016/j.nanoen.2015.06.029
2211-2855/

Introduction

An autonomous energy harvesting system with the capability of scavenging different forms of environmental renewable energy will undoubtedly improve its competitiveness in all end-use categories ranging from wearable consumer electronics [1], smart building [2] to grid-level energy production [3]. Solar and mechanical energies are two attractive forms [4–7]; however, most of the harvesting technologies that widely marketed are on basis of rigid and heavy body, such as single-crystal silicon solar cells and electromagnetic generators, which are incompatible with human body. Meanwhile, their unit-cost for the investments as well as the environmental payback time are not quite satisfactory. Solution processed devices for harvesting renewable energy can be fabricated by coating multiple functional layers on a polymer substrate directly, this kind of flexible, lightweight and inexpensive devices innovated the manufacture of improved efficiency with minimized environmental impacts and economic issues, and also boosted the development of wearable electronic system [8]. The printable organic solar cells (OSCs) thus were attracted intensive attentions [6,9]. However, the working mechanism of OSCs determines that they can only work when they are exposed to light, and the outputs would rapidly decrease when the intensity of irradiation reduced. Integrating extra unit, which is capable to harvest mechanical energy, with OSC is a feasible way to compensate this deficiency to a certain extent, overcoming the environmental limitations of single energy harvesting mode of the devices [10,11]. Xu et al. firstly demonstrated a hybrid cell that integrated dye-sensitized solar cell with a piezoelectric nanogenerator [12], and many recent research works extended the hybrid concept to the electromagnetic [13] and thermoelectric energies [14]; however, these rigid devices are difficult to be combined with flexible OSC.

The emerging polymer-based triboelectric nanogenerator (TENG) makes the integration possible [15,16], they are easy fabrication, cost-effective and lightweight. Moreover, TENG can efficiently convert various ambient renewable mechanical energies [17,18], such as irregular wave energy [19], wind energy [20] and biomechanical energy [21] into electric power utilizing triboelectric effect. However, the acceptability of TENG for the intergation highly depends on the transparency of it, to maximize the transparency could reduce the effect on the solar absorption of OSC along the visible region, leading to higher output power overall. Also, the synthetic method of TENG is preferred to be compatible with solution-based process.

Herein, we present a solution processed hybrid cell by integrating an OSC and a single-electrode triboelectric nanogenerator (STENG) into a flexible thin-film, as a wearable power source, the device is capable to harvest both of the solar and mechanical energies individually or simultaneously, breaking the environmental restrictions and complementarily utilizing available energy around the clock. This prototype offers a feasible approach for mass production of inexpensive power source, which can be roofed as household electric power supply even in the rainy day [22] or upgrade various wearable electronics, such as epidermal healthcare monitoring, which is always hidden under cloth, to get rid of the reliance on external power supply [23].

Experimental section

Preparation of silver nanowires (AgNWs)

AgNWs were synthesized using a modified polymer-mediated polyol process [24]. In detail, polyvinyl pyrrolidone (PVP) (0.26 g, MW=1,300,000) and $FeCl_3$ (0.15 mg) were dissolved in ethylene glycol (50 ml) under stirring. The solution was pre-heated at 180 °C for 30 min and cooled down to room temperature spontaneously. $AgNO_3$ (0.1168 g) was added into the solution until it completely dissolved, then the solution was sealed in a glass bottle and kept at 145 °C for 12 h in an oven. Afterwards, the as-prepared AgNWs were washed with acetone and ethanol for three times each, and re-dispersed in ethanol as AgNW ink.

Fabrication of transparent electrode, nanogenerator and hybrid cell

The conductive and transparent AgNWs/PI electrodes were fabricated via in-situ polymerization. AgNW ink was firstly coated on a silicon wafer using the Mayer-rod method, and the obtained AgNWs network on the wafer was annealed at 250 °C for 10 min to weld the junctions. The functional fluorinated PI precursor powder [25] was dissolved in dimethylacetamide (DMAc) as precursor solution (10 wt%), and coated it onto the as-prepared AgNWs network, then dried at 80 °C for 20 min and polymerized at 120 °C for 1 h in the oven. Afterwards, the transparent AgNWs/PI electrode can be peeled off. A STENG was fabricated by binding a transparent fluorinated ethylene propylene (FEP) film on the bare side of the AgNWs/PI using PI precursor.

The flexible OSC was constructed on the substrate of the as-prepared AgNWs/PI electrode. A 40 nm thick layer of modified PEDOT:PSS (Clevious P VP A1 4083) was firstly spun cast on the electrode, then annealed at 150 °C for 10 min in air. 2 nm thick layer of polyethylenimine (PEI, Aldrich, MW=25,000) was spin-coated on the PEDOT:PSS layer at a speed of 5000 r.p.m for 1 min, and annealed at 100 °C for 10 min in air. The PEI solution was prepared by dissolving the branched PEI in 2-methoxyethanol with a concentration of 0.4 wt%. Then, 70 nm of the active layer of poly(3-hexylthiophene) (P3HT, Lumtec):indene-C_{60} bis-adduct (ICBA, Lumtec) (P3HT:ICBA) (1:1, weight ratio, 24 mg/ml) was spin-coated upon the PEI layer at a speed of 1000 r.p.m for 40 s in a N_2 filled glovebox, and then annealed at 150 °C for 10 min. The top electrode of the solar cell was prepared by the transfer lamination technique that has been developed previously [26]. The hybrid cell was assembled by binding the STENG and OSC using a very thin PI layer to avoid short circuit.

Characterizations and measurements of the cells

The morphologies, structures and compositions of the samples were characterized by a scanning electron microscope (SEM, FEI Nova NanoSEM 450). The roughness of the conductive PI film was probed using an atomic force microscope (AFM, SPI 4000, Seiko). The optical transmittance

was measured using an ultraviolet-visible spectrometer (UV-vis, Shimadzu UV2550). Sheet resistance (R_s) was determined using a four-point probe resistivity measurement system. The output current of STENGs was measured by a low noise voltage preamplifier (Keithley 6514) while the output current was measured by a low-noise current preamplifier (Stanford Research SR560). The hybrid cell was fixed on a glass and measured in the glovebox, and the STENG was connected with OSC in parallel. The performances of sole STENGs of the hybrid cell with different AgNWs density were measured without any irradiation, using a resonator (JZK, Sinocera) with a covered cotton fabric to periodically trigger the STENG at the frequency of 4 Hz that controlled by a signal generator (YE 1311-D, Sinocera). The performance of hybrid cell was measured under the light intensity of 1000 W/m^2 (AM 1.5G) and ~2 W/m^2 (fluorescent light). To simulate the application of wearable electronics, a sparse cotton fabric was placed on the device to shield a portion of the light, one end of the cotton was fixed, and another end was shaken by hand to trigger the STENG, the output signal was rectified. Simultaneously, the light passed through the cotton fabric can be collected by OSC. The performances of the hybrid cell were measured by Keithley 2400.

Results and discussion

The layer-structured film of solution processed hybrid cell is flexible and semi-transparent. The schematic diagram in Figure 1a shows the view of exploded structure, and the upper inset shows the corresponding layout of the hybrid cell. Top STENG involves a 45 μm thick FEP film binding with a 55 μm thick AgNWs/PI electrode. Both of them are highly transparent in visible light spectrum, thus have little effect to the photoconversion efficiency of OSC. The bottom OSC was fabricated by sandwiched a 80 nm thick semi-transparent active layer of P3HT:ICBA between a 40 nm thick top electrode of modified PEDOT:PSS (PH1000) and 2 nm thick layer of electron-rich PEI [27], and settled them on the bottom electrode that prepared by coating 40 nm thick layer of PEDOT:PSS on the AgNWs/PI film. The total thickness of the hybrid cell is about 155 μm in this case, and can be easily adjusted according to the requirements, because it mainly depends on the thickness of PI substrate. Three dominant layers of the device can be clearly seen from the cross-sectional SEM image in lower inset of Figure 1a. The transmittance curve in Figure 1b indicates the active layer of OSC in the hybrid cell mainly absorbed the light in the wavelength of 400–550 nm, hence the device showed semi-transparent red (insets in Figure 1b). Compared with the rigid hybrid cells on basis of the inorganic materials [12,28], our device exhibits excellent flexibility (lower inset in Figure 1b), thus it is stimulated to apply as wearable power source.

The electrode as a key component of the hybrid cell ensures its stability, reliability and outstanding performance. They required high flexibility, high optical transmittance, low R_s, smooth surface and good mechanical stability. Comparing with other transparent conductive electrodes [29–33], recent developed electrodes based on AgNWs network can be simply prepared by coating of AgNW ink, exhibited more excellent performances [34]. However, not all the requirements were satisfied as following the reported methods, such as the slip and friction between of the AgNWs may break the electrode since the AgNWs only weakly anchored on the substrate by van der Waals force [35–37], it is conflict to apply the eletrode for TENG. We developed AgNWs/PI composite electrode to address these strict requirements. Figure 2a shows that the electrode is almost invisible by naked eyes with the R_s about 12 Ω/sq and optical transmittance of 92% at wavelength of 550 nm (Figure 2c). The relatively higher haze, compares to the traditional indium tin oxides (ITO) electrode [38,39], can be observed due to light scattering of AgNWs, it is helpful to enhance the photoconversion efficiency of the OSC. R_s are quite uniform with the standard deviation of 1.22 Ω/sq over the electrode as shown in Figure 2b, which is benefited from the mono-dispersion of AgNWs in the solvent, thus allows the uniform distribution of AgNWs (Figure 2d), and this

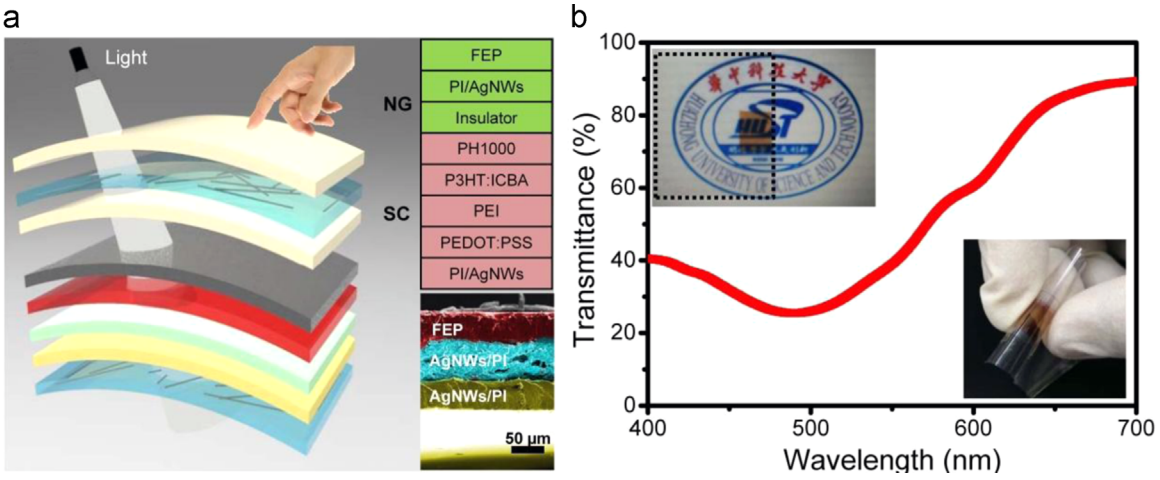

Figure 1 The design and layout of the hybrid cell. (a) Exploded view layout of the hybrid cell. The upper inset is the schematic illustration of the hybrid cell and the lower inset is the corresponding cross-sectional SEM image. (b) The optical transmittance of the hybrid cell. The upper inset shows the reddish semi-transparent hybrid area and high transparent STENG area, and the lower inset presents the flexibility of the hybrid cell.

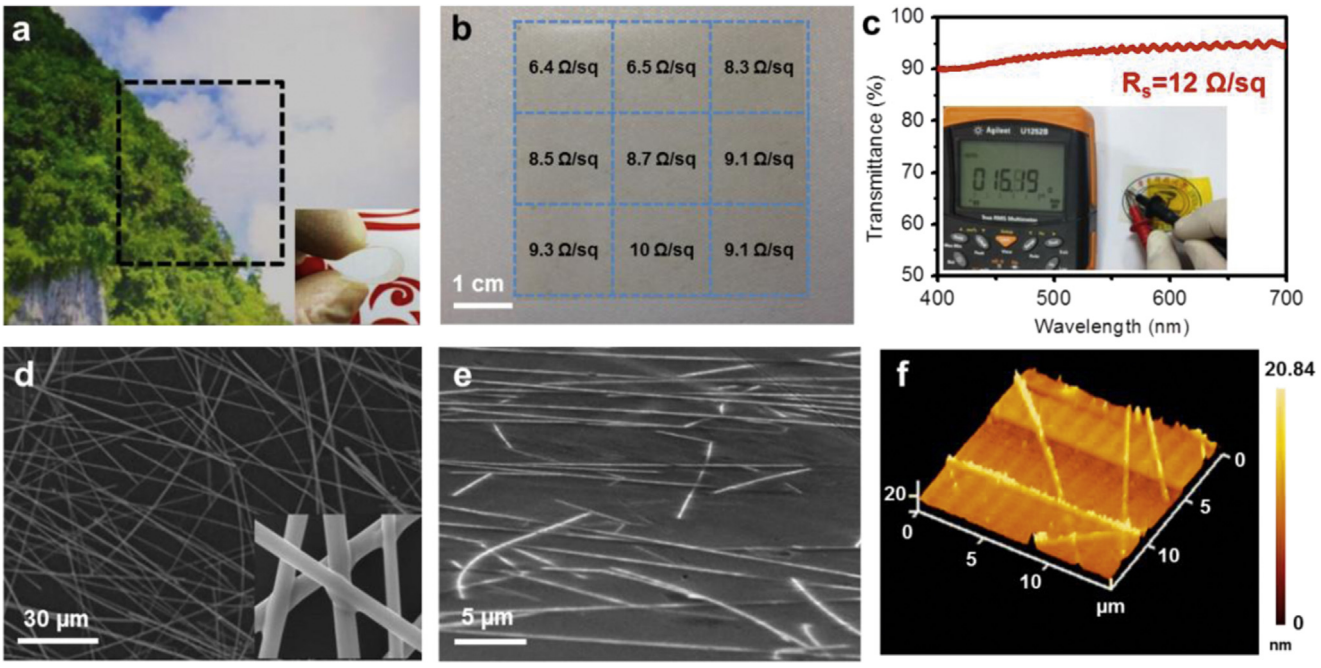

Figure 2 Characterizations of the AgNWs/PI electrode. (a) Photographs present the high transparent and flexible (inset) AgNWs/PI film. (b) Uniform R_s distribution on the AgNWs/PI electrode. (c) Plot of transmittance versus wavelength of AgNWs/PI electrode, and inset is the resistance measurement after scotch tape test. (d) SEM images of as-prepared AgNWs network and the welded junctions (inset). (e) The 45° titled SEM image of the AgNWs embedded in PI substrate. (g) AFM image of the surface roughness profile of the AgNWs/PI electrode.

value is acceptable for most of the optoelectronic applications [40]. The tightly welded junctions of AgNWs after annealing (inset in Figure 2d and Figure S1) effectively reduce the overall R_s, and the interconnections between the AgNWs can suppress the slip and friction if the substrate is bend. Compared with the strategy of directly coating AgNWs on the flexible substrate, the tightly gripped AgNWs by in-situ polymerized PI substrate significantly enhance the binding strength and improve the stability of the electrode. As seen in Figure 2c, Figure S2 and Movie in Supporting information, R_s even can be preserved after scotch tape test with the force about 4.3 N, it promises the mechanical stability of using the electrode for STENG. The tilted SEM view in Figure 2e shows that the AgNWs are embedded in PI but not immersed completely (Figure S3), and the roughness of the surface is about 10 nm as shown in AFM image (Figure 2f). This composite structure cannot only ensure the conductivity of the surface, but also prevent the short circuit, when it is used as the electrode of OSC, because the thickness of the active layer is typically in a few tens of nanometers. Hence, the AgNWs/PI is a qualified electrode for hybrid cell, and potentially can be used in more restrict conditions [41].

The hybrid cell was fabricated by binding the STENG and OSC using a very thin PI layer as described in *Experimental section*, and each unit can work independently. The hybrid cell work without light irradiation is demonstrated in Figure 3, thus all the electric power was contributed from STENG. For simulating the process of mechanical energy input, STENG was triggered using a cotton fabric that is fixed on a resonator to touch the FEP film periodically with the frequency of 4 Hz, (different substances such as fingers, theoretically, even water drops [42] can be used to generate power, but the output performance would vary). The working mechanism illustrated in Figure S4 has been studied in previous work [21] and can be briefly described as following. The process of generating electric power can be identified into four stages. Initially, the cotton fabric tightly contacts with the FEP film (Figure S4a), since FEP is more triboelectrically negative than cotton, the FEP is able to acquire the electrons from the cotton fabric under the contact electrification [16], and the system is in equilibrium by then without any charge transfers in the external circuitry. Following that, the cotton fabric begins to separate from FEP film (Figure S4b), and the uncompensated negative charges on FEP film would electrostatically induce the positive charges in the bottom AgNWs electrode to neutralize partial negative charges. This process drives the free electrons in AgNWs to the ground to induce current until the cotton fabric is completely removed (Figure S4c) [43]. In turn, the approached cotton fabric is able to neutralize the negative charges on the FEP film again, resulting in the electrons flow back to the AgNWs electrode from the ground (Figure S4d), and the typical current density is presented in Figure S5. In this sense, the cycles can be repeated utilizing external objects as a pump to drive the electrons up and down.

Compared with previous TENGs using sputter-coated metallic film as the electrodes [16,44], a different mechanism is involved in this transparent unit, because there is a trade-off between the output performance and the transmittance of the STENG. The output performance significantly depends on the density of AgNWs in the electrode, which also determines the transmittance of the electrode.

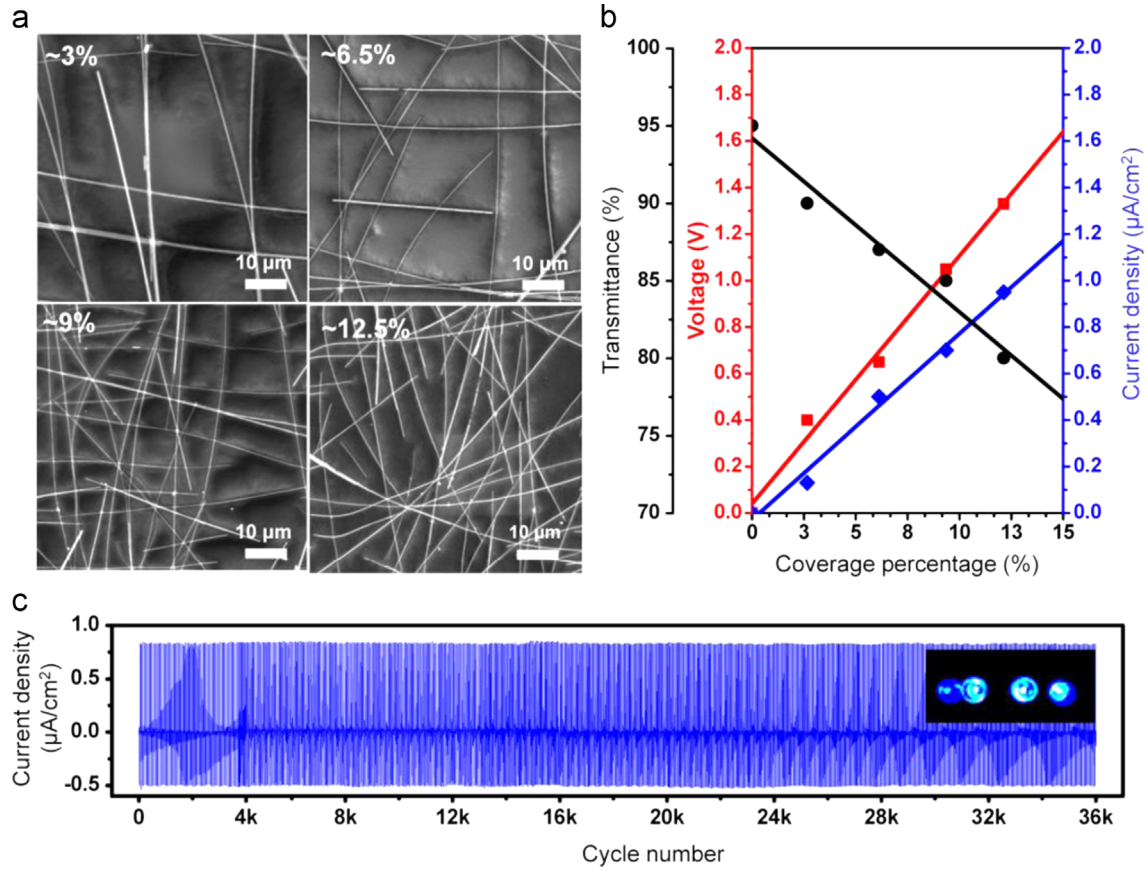

Figure 3 Relationship between AgNWs/PI electrode and the performance of STENG in the hybrid cell without light irradiation. (a) The SEM images of AgNWs/PI electrode with the coverage percentages of AgNWs correspond to 3%, 6.5%, 9% and 12.5%. (b) The optical transmittance, J_{sc} and V_{oc} of STENG are plotted as a function of coverage percentage. (c) The stability of the STENG. The inset shows 4 commercial LED bulbs can be lit up solely using the STENG that has transmittance of 85%.

The density of the AgNWs can be adjusted by control the deposition times of AgNW ink, SEM images in Figure 3a clearly show that the density of AgNWs in PI substrate is proportional to the deposition times of AgNW ink (considering the distribution of AgNWs is uniform, and the coverage area can be caculated from the typical SEM images when assuming the average diameter of AgNW is 100 nm), and the optical transmittance, output voltage and current are plotted as a function of the coverage percentage of the AgNWs in Figure 3b. The output voltage and current gradually increase with enlarging the coverage area of AgNWs from around 3% to 12.5%, the short circuit current (J_{sc}) increases from 0.15 to 0.95 μA/cm^2, while the open-circuit voltage (V_{oc}) increases from 0.4 to 1.25 V, respectively. Both of them increase linearly as seen from the fitted lines, this is due to that the sparse AgNWs network restricts the density of induced positive charges, in another words, increased density of the AgNWs leads more conductive paths that can acquire more positive charges, thus enhancing output performance. This result is further proved by comparing with the STENG using sputter coating Ag film on the PI substrate as the electrode, for which J_{sc} increased to 3.8 μA/cm^2 (Figure S6a), while no signal is observed with a bare PI film in Figure S6b. However, an opposite tendency of the optical transmittance from 91% to 80% can be observed with the increase of the coverage area of AgNWs gradually, which indicates that the increase of the density of AgNWs can improve the output at the expense of optical transmittance. However, as the STENG is designed as the upper surface in the hybrid cell, it must be transparent enough to ensure the light absorption of the bottom OSC. Thus, the STENG has optical transmittance around 85% was used for the further study. In addition, the STENG exhibits excellent working stability as demonstrated in Figure 3c. The output has no degradation during the fatigue test of 35,000 cycles indicating the extremely long working life of the STENG [45], a unit of 4 commercial light-emitting diode (LED) bulbs can be lit up twice in each cycle solely using STENG (inset in Figure 3c).

The synergetic behavior for harvesting the renewable energies by superposing the energy of the outputs from STENG and OSC indeed demonstrates the advantages of hybrid cell as seen in Figure 4. Towards the applications of wearable power supply, this flexible hybrid cell is inevitably used in the indoor condition with weak light, even would be covered by cloth such as the healthcare applications, as schematically illustrated in Figure 4a. The photons can pass through the clothing fabrics (cotton fabric in our study) and the transparent STENG to reach the active layer of OSC for photovoltaic reaction. Simultaneously, the fabric would touch the STENG irregularly to convert the biomechanical motion energy into electric power when the body moves. The typical current density versus voltage (J-V) curves of the hybrid cell without input of STENG are demonstrated

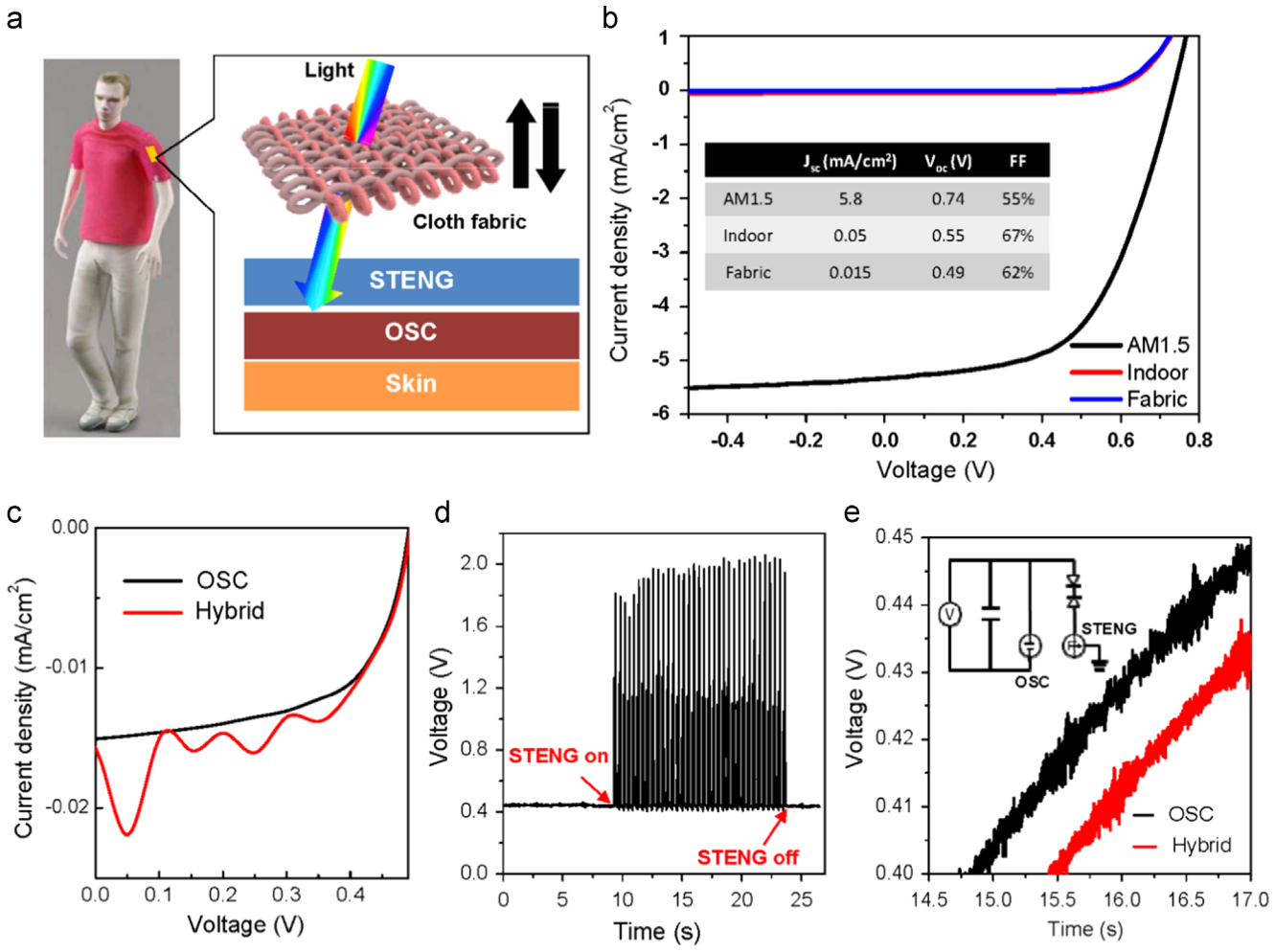

	J_{sc} (mA/cm²)	V_{oc} (V)	FF
AM1.5	5.8	0.74	55%
Indoor	0.05	0.55	67%
Fabric	0.015	0.49	62%

Figure 4 Performances of the hybrid cell. (a) Schematic illustration of the working mechanism of the hybrid cell hidden under the cloth fabric as wearable power source. (b) Comparison of *J*–*V* characterization of hybrid cell under simulated AM 1.5G irradiation (intensity of 1000 W/m^2), standard indoor fluorescent lighting (2 W/m^2) with and without cover of cotton fabric. (c) Comparison of *J*–*V* curve of sole OSC and hybrid cell under indoor lighting, in which the STENG was triggered by shaking the fabric. (d) The output voltage of sole OSC and hybrid cell with and without STENG. (d) The time spent to charge a 10 μF commercial capacitor using the hybrid cell with and without STENG input. The inset depicts the equivalent loop circuit for storing the electrical energy that produced by the hybrid cell.

under different light irradiation conditions as shown in Figure 4b, including simulated AM 1.5G irradiation (intensity of 1000 W/m^2), standard indoor fluorescent lighting (2 W/m^2) with and without the cover of the cotton fabric. The efficiency of sole OSC is 2.4% with the J_{sc} of 5.8 mA/cm^2, V_{oc} of 0.74 V and fill factor (FF) of 55% under the simulated AM 1.5 G irradiation, and the performance can be further improved by increasing thickness of active layer, but the total transmittance of the hybrid cell would decrease. In this situation, the output performance of the hybrid device is dominated by the OSC and the output of STENG is negligible. However, J_{sc} of the OSC dramatically decreases to 0.05 mA/cm^2 under standard indoor fluorescent lighting as seen in the inset table of Figure 4b, and as low as 0.015 mA/cm^{2}when it was covered with the fabric. These results implied that when the OSC is used in weak light or as a power source for wearable electronic devices which are attached on the skin and always covered by cloth, harvesting the other forms of energy for compensation is necessary.

As demonstrated in Figure 4c, *J*-*V* curve of the OSC of the hybrid cell exhibits notable enhancement under the room light when the STENG is activated simultaneously. The pulse energy scavenged from the repeated contacts between cotton fabric and STENG is superimposed upon the *J*-*V* curve of OSC. In this case, the contributed share of STENG in the hybrid cell is significant and comparable with OSC.

The synergetic behavior of the hybrid cell is further identified through the time-dependent behavior of output voltage as shown in Figure 4d, because the two units were connected in parallel, the output voltage of the hybrid cell is entirely determined by the unit that has higher output voltage between them. The steady output voltage of OSC, when it was covered with the fabric, is around 0.45 V under indoor light, when the STENG is triggered by shaking the fabric, the outputs voltage of the hybrid cell can get the pulse peak value up to ~1.9 V. This result further proves that the unit in hybrid cell cannot only work independently to compensate the deficiency of sole energy harvesting

mode, but also enhance output if both units are available. The practical application of the hybrid cell is demonstrated through a time-comparison of charging a commercial capacitor (10 μF) using sole OSC and fully functioned hybrid cell as shown in Figure 4e, the equivalent loop circuit as used for charging the capacitor is illustrated as the inset of Figure 4e. The duration to charge the capacitor is obviously shorter when fully activating the hybrid cell than solely using the OSC, proving that the hybrid system is a more effective power generator than any single unit in it, which provides a truly feasible way to charge other flexible energy storage units such as batteries and supercapacitors. This semi-transparent energy device can also be pasted on the glass windows to harvest different forms of energy from sunlight, rain drop [40] and indoor light at night, if the devices can be well packaged.

Conclusion

In summary, we present an all solution processed hybrid energy harvesting system by integrating the STENG and OSC in a thin film, in which the excellent AgNWs/PI electrodes enable the flexibility and mechanical stability of the device. The as-fabricated hybrid cell is capable to convert both of the solar and mechanical energies into electricity independently or simultaneously, and the contributed share from STENG is significantly increased in the weak light conditions. The synergetic energy harvesting behavior provides a feasible way to solve the environmental limitation of single energy supply mode. According to this prototype, the other flexible and transparent TENGs on basis of graphene [46], carbon nanotubes or organic conductor can also be developed for hybrid system. Moreover, other ambient energy harvesting units such as thin film thermoelectric generator [47] can also be integrated into the hybrid cell to further enhance the output power, consequently the application areas can be enormously expanded [48], like epidermal electronics, which was quite restricted by external power source for full-time healthy monitoring.

Acknowledgments

YXF and JHT contributed equally to this work. The work was supported by the National Natural Science Foundation of China (Nos.: 61204001, 61307026, 51202076), Frontier and Key Technological Innovation Special Foundation of Guangdong Province (2014B090915001), the Fundamental Research Funds for the Central Universities of China (2014QN013), the Natural Science Foundation of Hubei Province (2015CFB312). The authors thank the facility support of the Center for Nanoscale Characterization & Devices (CNCD), and the helps from Guoli Tu and Bo Wang in WNLO of HUST.

Appendix A. Supplementary information

Supplementary data associated with this article can be found in the online version at doi:10.1016/j.nanoen.2015.06.029.

References

[1] K. Nomura, H. Ohta, A. Takagi, T. Kamiya, M. Hirano, H. Hosono, Nature 432 (2004) 488–492.
[2] C.G. Granqvist, Sol. Energy Mater. Sol. Cells 91 (2007) 1529–1598.
[3] J. Chen, J. Yang, Z. Li, X. Fan, Y. Zi, Q. Jing, H. Guo, Z. Wen, K.C. Pradel, S. Niu, Z.L. Wang, ACS Nano 9 (2015) 3324–3331.
[4] Q.Z. Zhong, J.W. Zhong, B. Hu, Q.Y. Hu, J. Zhou, Z.L. Wang, Energy Environ. Sci. 6 (2013) 1779–1784.
[5] W. Wu, L. Wang, Y. Li, F. Zhang, L. Lin, S. Niu, D. Chenet, X. Zhang, Y. Hao, T.F. Heinz, J. Hone, Z.L. Wang, Nature 514 (2014) 470–474.
[6] C.C. Chen, L.T. Dou, R. Zhu, C.H. Chung, T.B. Song, Y.B. Zheng, S. Hawks, G. Li, P.S. Weiss, Y. Yang, ACS Nano 6 (2012) 7185–7190.
[7] G.J. Snyder, E.S. Toberer, Nat. Mater. 7 (2008) 105–114.
[8] B. Hu, Y. Ding, W. Chen, D. Kulkarni, Y. Shen, V.V. Tsukruk, Z.L. Wang, Adv. Mater. 22 (2010) 5134–5139.
[9] J.S. Luo, J.H. Im, M.T. Mayer, M. Schreier, M.K. Nazeeruddin, N.G. Park, S.D. Tilley, H.J. Fan, M. Gratzel, Science 345 (2014) 1593–1596.
[10] M. Han, X.-S. Zhang, B. Meng, W. Liu, W. Tang, X. Sun, W. Wang, H. Zhang, ACS Nano 7 (2013) 8554–8560.
[11] M.D. Han, X.S. Zhang, X.M. Sun, B. Meng, W. Liu, H.X. Zhang, Sci. Rep. UK 4 (2014) 4811.
[12] C. Xu, X.D. Wang, Z.L. Wang, J. Am. Chem. Soc. 131 (2009) 5866–5872.
[13] A. Collado, A. Georgiadis, IEEE Trans. Circuits-I 60 (2013) 2225–2234.
[14] D.J. Yang, H.M. Yin, IEEE Trans. Energy Convers. 26 (2011) 662–670.
[15] Y.N. Xie, S.H. Wang, S.M. Niu, L. Lin, Q.S. Jing, J. Yang, Z.Y. Wu, Z.L. Wang, Adv. Mater. 26 (2014) 6599–6607.
[16] F.R. Fan, Z.Q. Tian, Z. Lin Wang, Nano Energy 1 (2012) 328–334.
[17] C.K. Jeong, K.M. Baek, S.M. Niu, T.W. Nam, Y.H. Hur, D. Y. Park, G.T. Hwang, M. Byun, Z.L. Wang, Y.S. Jung, K.J. Lee, Nano Lett. 14 (2014) 7031–7038.
[18] S.H. Lee, C.K. Jeong, G.-T. Hwang, K.J. Lee, Nano Energy 14 (2014) 111–125.
[19] G. Zhu, Y.J. Su, P. Bai, J. Chen, Q.S. Jing, W.Q. Yang, Z.L. Wang, ACS Nano 8 (2014) 6031–6037.
[20] J. Bae, J. Lee, S. Kim, J. Ha, B.S. Lee, Y. Park, C. Choong, J.B. Kim, Z.L. Wang, H.Y. Kim, J.J. Park, U.I. Chung, Nat. Commun. 5 (2014) 4929.
[21] Y. Yang, H.L. Zhang, Z.H. Lin, Y.S. Zhou, Q.S. Jing, Y.J. Su, J. Yang, J. Chen, C.G. Hu, Z.L. Wang, ACS Nano 7 (2013) 9213–9222.
[22] L. Zheng, Z.H. Lin, G. Cheng, W.Z. Wu, X.N. Wen, S.M. Lee, Z.L. Wang, Nano Energy 9 (2014) 291–300.
[23] J.W. Zhong, Y. Zhang, Q.Z. Zhong, Q.Y. Hu, B. Hu, Z.L. Wang, J. Zhou, ACS Nano 8 (2014) 6273–6280.
[24] S.W. Zhu, Y. Gao, B. Hu, J. Li, J. Su, Z.Y. Fan, J. Zhou, Nanotechnology 24 (2013) 335202.
[25] T. Hasegawa, K. Horie, Prog. Polym. Sci. 26 (2001) 259–335.
[26] Y.H. Zhou, T.M. Khan, J.W. Shim, A. Dindar, C. Fuentes-Hernandez, B. Kippelen, J. Mater. Chem. A 2 (2014) 3492–3497.
[27] Y.H. Zhou, C. Fuentes-Hernandez, J. Shim, J. Meyer, A.J. Giordano, H. Li, P. Winget, T. Papadopoulos, H. Cheun, J. Kim, M. Fenoll, A. Dindar, W. Haske, E. Najafabadi, T.M. Khan, H. Sojoudi, S. Barlow, S. Graham, J.L. Bredas, S.R. Marder, A. Kahn, B. Kippelen, Science 336 (2012) 327–332.
[28] Y. Yang, H.L. Zhang, Z.H. Lin, Y. Liu, J. Chen, Z.Y. Lin, Y.S. Zhou, C.P. Wong, Z.L. Wang, Energy Environ. Sci. 6 (2013) 2429–2434.
[29] K. Ando, S. Watanabe, S. Mooser, E. Saitoh, H. Sirringhaus, Nat. Mater. 12 (2013) 622–627.

[30] S. Hong, S. Myung, Nat. Nanotechnol. 2 (2007) 207–208.
[31] H. Kang, S. Jung, S. Jeong, G. Kim, K. Lee, Nat. Commun. 6 (2015) 6503.
[32] H. Dong, Z.X. Wu, F. Lu, Y.C. Gao, A. El-Shafei, B. Jiao, S.Y. Ning, X. Hou, Nano Energy 10 (2014) 181–191.
[33] B. Han, K. Pei, Y. Huang, X. Zhang, Q. Rong, Q. Lin, Y. Guo, T. Sun, C. Guo, D. Carnahan, M. Giersig, Y. Wang, J. Gao, Z. Ren, K. Kempa, Adv. Mater. 26 (2014) 873–877.
[34] M.S. Lee, K. Lee, S.Y. Kim, H. Lee, J. Park, K.H. Choi, H.K. Kim, D.G. Kim, D.Y. Lee, S. Nam, J.U. Park, Nano Lett. 13 (2013) 2814–2821.
[35] H. Wu, D. Kong, Z. Ruan, P.C. Hsu, S. Wang, Z. Yu, T.J. Carney, L. Hu, S. Fan, Y. Cui, Nat. Nanotechnol. 8 (2013) 421–425.
[36] B. Zhang, Z.M. Xiang, S.W. Zhu, Q.Y. Hu, Y.Z. Cao, J.W. Zhong, Q.Z. Zhong, B. Wang, Y.S. Fang, B. Hu, J. Zhou, Z.L. Wang, Nano Res. 7 (2014) 1488–1496.
[37] J.W. Liu, J.L. Wang, Z.H. Wang, W.R. Huang, S.H. Yu, Angew. Chem. Int. Ed. 53 (2014) 13477–13482.
[38] Z.Q. Fang, H.L. Zhu, Y.B. Yuan, D. Ha, S.Z. Zhu, C. Preston, Q.X. Chen, Y.Y. Li, X.G. Han, S. Lee, G. Chen, T. Li, J. Munday, J.S. Huang, L.B. Hu, Nano Lett. 14 (2014) 765–773.
[39] T. Araki, J. Jiu, M. Nogi, H. Koga, S. Nagao, T. Sugahara, K. Suganuma, Nano Res. 7 (2014) 236–245.
[40] Y. Zhao, D. Nothern, A. Yadav, K.-H. An, K.P. Pipe, M. Shtein, Org. Electron. 15 (2014) 3529–3537.
[41] M. Kaltenbrunner, T. Sekitani, J. Reeder, T. Yokota, K. Kuribara, T. Tokuhara, M. Drack, R. Schwoediauer, I. Graz, S. Bauer-Gogonea, S. Bauer, T. Someya, Nature 499 (2013) 458–463.
[42] Z.H. Lin, G. Cheng, S. Lee, K.C. Pradel, Z.L. Wang, Adv. Mater. 26 (2014) 4690–4696.
[43] G. Zhu, J. Chen, Y. Liu, P. Bai, Y.S. Zhou, Q. Jing, C. Pan, Z.L. Wang, Nano Lett. 13 (2013) 2282–2289.
[44] G. Zhu, Y.S. Zhou, P. Bai, X.S. Meng, Q.S. Jing, J. Chen, Z.L. Wang, Adv. Mater. 26 (2014) 3788–3796.
[45] Y. Li, G. Cheng, Z.-H. Lin, J. Yang, L. Lin, Z.L. Wang, Nano Energy 11 (2015) 323–332.
[46] S. Kim, M.K. Gupta, K.Y. Lee, A. Sohn, T.Y. Kim, K.S. Shin, D. Kim, S.K. Kim, K.H. Lee, H.J. Shin, D.W. Kim, S.W. Kim, Adv. Mater. 26 (2014) 3918–3925.
[47] S.J. Kim, J.H. We, B.J. Cho, Energy Environ. Sci. 7 (2014) 1959–1965.
[48] B. Hu, W. Chen, J. Zhou, Sens. Actuators B Chem. 176 (2013) 522–533.

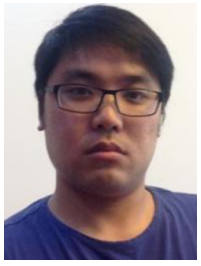

Yuanxing Fang received his Master of Chemistry degree in University of Sussex, United Kingdom in 2012. He is a Ph.D. candidate at Chemistry Department, University of Sussex. From 2014 to 2015, he was as a visiting student in Wuhan National Laboratory for Optoelectronics, and school of Optical and Electronics Information, Huazhong University of Science and Technology, China. His research interests are synthesis and characterization of novel nanostructured functional materials, and preparation the devices for the applications of triboelectric nanogenerators, solar cells and photoelectrochemical cells.

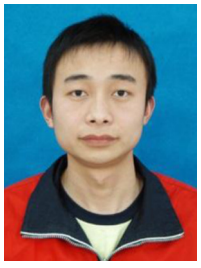

Jinhui Tong received his B.S. degree in Electronic Science and Technology from Hubei University, PR China in Jun, 2010. He is a Ph.D. candidate in Wuhan National Laboratory for Optoelectronics (WNLO) at HUST. His research interests include organic-inorganic tandem solar cells.

Qize Zhong received his B.S. degree in Optoelectronic Information from Huazhong University of Science and Technology (HUST), PR China in Jun, 2011. He is a Ph. D. candidate in Wuhan National Laboratory for Optoelectronics (WNLO) and School of Optical and Electronic Information at HUST. His research interests include flexible electronics.

Dr. Qiao Chen obtained his Ph.D. degree in Physical Chemistry at the IRC in Surface Science at Liverpool University in 1994. He joined London Centre for Nanotechnology at the University College London (2003–2007) before he took a lectureship in Physical Chemistry at the University of Sussex. He has over 75 publications in the field of nanotechnology and surface chemistry. His recent research interest is focused on photocatalytic properties of nanomaterials, with particular applications in environment remediation, green energy and in addition to heterogeneous catalysis and surface chemistry in general.

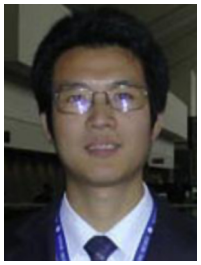

Dr. Jun Zhou received his B.S. degree in Material Physics (2001) and his Ph.D. in Material Physics and Chemistry (2007) from Sun Yat-Sen University, China. During 2005–2006, he was a visiting student in Georgia Institute of Technology. After obtaining his Ph.D., he worked in Georgia Institute of Technology as a research scientist. He joined in Wuhan National Laboratory for Optoelectronics (WNLO), Huazhong University of Science and Technology (HUST) as a professor from the end of 2009. His main research interest is flexible energy harvesting and storage devices.

Dr. Qiuping Luo received her Ph.D. degree in the School of Chemistry and Chemical Engineering in 2012, Sun-Yat Sen University, PR China. She is a postdoc in Wuhan National Laboratory for Optoelectronics (WNLO) now. Her main research interest is focusing on the fabrication of nanomaterials and their applications in photochemistry and supercapacitors.

Dr. Yinhua Zhou received his bachelor (2003) and Ph.D. (2008) degree both from Jilin University, China. During his Ph.D. study, he spent one year in Prof. Olle Inganäs group as a visiting Ph.D. student in 2007–2008. After that, he worked as postdoctoral fellow in the Georgia Institute of Technology from 2009 to 2013 with Prof. Bernard Kippelen. Since October of 2013, he started the current position as a faculty member in Wuhan National Laboratory for Optoelectronics, Huazhong University of Science and Technology. His research interest includes conducting polymers, organic photovoltaics and printed electronics.

Dr. Zhong Lin (ZL) Wang is the Hightower Chair in Materials Science and Engineering, Regents' Professor, Engineering Distinguished Professor and Director, Center for Nanostructure Characterization, at Georgia Tech. Dr. Wang is a foreign member of the Chinese Academy of Sciences, fellow of American Physical Society, fellow of AAAS, fellow of Microscopy Society of America, and fellow of Materials Research Society. His discovery and breakthroughs in developing nanogenerators establish the principle and technological road map for harvesting mechanical energy from environment and biological systems for powering a personal electronics.

Dr. Bin Hu received his Ph.D. in materials science at Wuhan University of Technology in 2011. From 2009–2011, he was a visiting student in Georgia Institute of Technology. He joined in Wuhan National Laboratory for Optoelectronics (WNOL) from 2012 as an associate professor, and his main research interest is the flexible optoelectronic devices for integrated self-powered nano- and microsystems.